

## Structural Response Analysis of Experimentally Tested Aluminum Cracked Panels under Compressive Load

Ashraf Attia<sup>1</sup>, \*, S. Saad-Eldeen<sup>1</sup>, Mostafa M. EL-Afandy<sup>2</sup>, Heba S. El-kilani<sup>1</sup>

<sup>1</sup>Department of Naval Architecture and Marine Engineering, Port said university, Egypt, email: [a.abdelhady@eng.psu.edu.eg](mailto:a.abdelhady@eng.psu.edu.eg)

<sup>1</sup>Department of Naval Architecture and Marine Engineering, Port said university, Egypt, email: [Saad.bahey@eng.psu.edu.eg](mailto:Saad.bahey@eng.psu.edu.eg)

<sup>1</sup>Department of Naval Architecture and Marine Engineering, Port said university, Egypt, email: [Hebaelkilani@eng.psu.edu.eg](mailto:Hebaelkilani@eng.psu.edu.eg)

<sup>2</sup> Egyptian Navy Shipyards, Alexandria, Egypt, email: [Melafandy@yahoo.com](mailto:Melafandy@yahoo.com)

\*Ashraf Attia, [a.abdelhady@eng.psu.edu.eg](mailto:a.abdelhady@eng.psu.edu.eg), DOI: [10.21608/PSERJ.2022.133315.1178](https://doi.org/10.21608/PSERJ.2022.133315.1178)

Received 13-4-2022

Revised 30-4-2022

Accepted 8-5-2022

© 2022 by Author(s) and PSERJ.

This is an open access article licensed under the terms of the Creative Commons Attribution International License (CC BY 4.0).

<http://creativecommons.org/licenses/by/4.0/>



### ABSTRACT

An experimental investigation is carried out to evaluate the ultimate compressive capacity of welded stiffened aluminum panels in alloy 5083-H116 subjected to uniaxial compressive load along the short edge. A tensile test is carried out to find out the real material properties. Five full-scale stiffened panel specimens, one of them is intact and locked cracks are produced in the other four panels. A global survey of the initial geometric imperfections is performed before conducting the compressive test. Through-thickness-locked cracks are located either in the center or quarter of the plate between the two attached stiffeners. The panels are tested, and their progressive collapse behavior is reported. The panels failed by two different deformation modes: stiffener tripping and local buckling of the plate. The load-shortening and load-lateral displacement relations are presented, and concluding remarks are stated regarding the effect of locked crack's location, orientation, and initial imperfection on the compressive capacity of welded aluminum panels.

**Keywords:** Experiment; panels; Aluminum; Cracks; Compressive load; Structural Response

## 1. INTRODUCTION

The beginning of aluminum usage in marine application was in the late 1890s, and the production of 5xxx (AL-Mg) alloys in the 1920s opened the door for the wide range usage of aluminum alloys in marine applications. Aluminum alloys are now acknowledged as the best in shipbuilding and production of components for offshore platforms, because of their distinguished mechanical properties. Ships and boats with high-speed capability and long-life cycle are designed by using aluminum alloys. The use of high-strength aluminum alloys in shipbuilding has a lot of advantages, but it also has a lot of drawbacks. Lighter weight, which helps enhance cargo capacity and lower power requirements, low density, high corrosion resistance, and inexpensive maintenance are

all advantages of aluminum compared to steel, [1]. However, the structural longevity of aluminum alloys is somewhat like that of steel when affected by cracking damage. In fact, cracks of various sizes and orientation may arise in ship plates, stiffened panels, and box girders at several locations during production or operating conditions. Many reasons can lead to cracking damage, such as local stress concentration, pitting corrosion, impact load, and welding defects, and it is essential to evaluate its influence on the ultimate strength of various ship structural members. Most of the experimental studies dealing with this issue are concerned with steel stiffened panels as the work done by Saad eldeen et al [2] who carried out experimental compressive tests on thin steel plates with a central elliptic opening accompanied by locked cracks of different

lengths. It was concluded that by increasing the crack length, the ultimate strength of steel plate with an opening is decreased. Also, the toughness and the dissipated energy up to ultimate strength decreases. Another experimental work by Saad eldeen [3] studied the combined effect of opening, cracks, and corrosion degradation on the structural behavior of rectangular steel plates through a group of experimental tests. It was concluded that, the increase of steel plate's thickness which has the same opening size and crack lengths, increases the ultimate strength of the plate. For plates of the same opening diameter and thickness, increasing in crack length by 20% has less effect on the overall load carrying capacity than decreasing the original imperfection amplitude by 37.5%.

A series of panels with an initial deformation and crack damage under uniaxial compressive loading was tested experimentally by Shi et al [4] where the ultimate strength of crack-damaged stiffened plates was assessed. The crack location, length, and angle between the crack and the longitudinal stiffener were verified. It was concluded that, the initial deformation decreases the load carrying capacity of the panel. Also, the various cracks angle may affect the stress distribution of panels. Zhang et al [5] analyzed experimentally and numerically the ultimate strength characteristics of panels with a crack and artificial pits under compressive load. A series of numerical analyses was conducted with different models for assessment the reduction in the ultimate strength by varying the location between crack tips and pits. It was concluded that due to the presence of crack and pitting in the panels, the reduction in the final strength is greater than that of the panels with crack or pitting only. Also, the distance between the crack and the pits has a major effect on the ultimate strength. Yu et al [6] studied the ultimate strength features of stiffened panels with cracks under longitudinal compression load. The influence of different geometrical features of cracks was considered, especially

the location of cracks. It was concluded that, the crack location has a remarkable effect on the reduction of ultimate strength of stiffened panels.

The residual ultimate strength under axial compressive loading of stiffened panels with locked cracks was numerically analyzed by Xu et al [7]. It was concluded that when the aspect ratio of the panel increases, the load carrying capacity decreases, and the angular cracks have a significant effect on the ultimate strength. The location of longitudinal cracks in the transverse direction is not a main factor and the residual ultimate strength of the stiffened panel can be affected slightly. The ultimate strength of stiffened panels with various crack length, crack position, plate thickness, and size of stiffeners, were studied numerically by Rahbar et al [8]. It was found that; the reduction in ultimate strength for thick plate in case of edge crack is higher than center crack. Stiffener type has no effect on the ultimate strength for thin plates, but for thick plate the ultimate strength reduction is higher in case of weaker stiffener.

Regarding aluminum alloy panels, Aalberg et al [9] carried out experimental tests on aluminum stiffened panels (AA6082); a total of 21 panels were made from extruded aluminum profiles connected by welding and tested under compressive load. They observed that, in case of closed section panels the collapse mode is a regular flexural buckling in the inner panels. For panels with open sections (L-shaped), the buckling initiation occurred by the stiffener tripping. A numerical investigation studied the influence of welding methods of extruded and non-extruded T-bar aluminum panels 6082-T6 on the ultimate strength, by Farajkhah et al [10]. The aluminum panels were joined by FSW, MIG butt, and MIG fillet welding. It was found that the non-extruded panels fabricated by MIG fillet welding have a lower load carrying capacity than the extruded stiffened plates joined by FSW method by 26%. The extruded panels joined by MIG butt welding have a lower

buckling load than that joined by FSW by 9%. Actually, in a recent review of the published work concerned with the ultimate strength of aluminum plates, panels, and ship hull girders [11], it was concluded that there is an interest for studying the extruded aluminum panels which reduce the initial imperfections induced by the welding process. The review stated that the experimental and numerical studies for unstiffened aluminum plates, and ship hull girders are very few, whereas the studies concerned with the ultimate strength of aluminum stiffened plates are available in abundance. Paik et al [1] studied experimentally and numerically the collapse mode behavior of welded aluminum stiffened panels under compression load. The effect of the initial imperfections on the ultimate limit state of the tested panels was studied. Based on the experimental and numerical results, a formula for investigation the ultimate limit state was derived. Liu et al [12] studied numerically the ultimate strength of aluminum and steel panels with openings on the girders. The effect of openings, heat affected zone, and boundary conditions were considered. They found that the considered aluminum panels can withstand higher load carrying capacity than the steel panels. The shape of the opening, size and position has a clear effect on the ultimate strength of the panels, and the best ultimate strength is achieved when the opening is located far away the flange of the girder. Also, the boundary conditions have a significant effect on the buckling behavior and the ultimate compressive load of the panels. Duan et al [13] investigated experimentally the response of aluminum alloy plates with and without initial cracks under repeated impact loading considering the length and depth of crack. It was found that with longer cracks as well as deeper crack, the deformation of plates increased. Attia et al. [14] carried out a recent review on the studies dealing with the effect of cracks on the ultimate strength of ship panels. It has been noticed that an experimental work dealing with the effect of locked cracks on the compressive ultimate strength of aluminum

panels needs more attention and such a study would be helpful to decide repair requirements. Therefore, the present study is a full-scale experimental work in the way to fill this gap. The progressive collapse and the load carrying capacity of various cracked aluminum welded stiffened panels under uniaxial compressive load are examined to detect the effect of crack location and orientation as well as the developed initial imperfections.

## 2. DESTRUCTIVE TESTS

To find out the actual compressive capacity of stiffened panels, two destructive tests are to be carried out. The first one is the tensile test, which correctly identify the mechanical properties of the constructing material of such stiffened panels. The second test is the compressive test that evaluates the ultimate compressive capacity of the stiffened panel with specific geometrical configurations. Both tests have been carried out at Structure and Concrete Research Laboratory, Faculty of Engineering, Port Said University.

### 2.1. Tensile Test

The used material in this study is aluminum alloy 5083-H116. A tensile test is carried out on a rectangular test coupon (400x30x6 mm) with gauge length of 200 mm as shown in Figure 1 (left) to obtain the actual mechanical properties of the material. A strain gauge is fitted in the mid of the test coupon, see Figure 1(left), to obtain accurate strain values during the test. The engineering stress-strain and the true stress- strain curves are plotted in Figure 1 (right). The values of the true stress and true strain can be derived in terms of the engineering stress and engineering strain using the following equations [15]:

$$\sigma_T = \sigma_e (1 + \varepsilon_e) \quad (1)$$

$$\varepsilon_T = \ln (1 + \varepsilon_e) \quad (2)$$

Where,  $\sigma_T$  is the true stress,  $\sigma_e$  the engineering stress,  $\varepsilon_e$  the engineering strain, and  $\varepsilon_T$  the true strain. The summary of the achieved mechanical properties as are given in Table 1. The aim of conducting such

compressive test is to find out the ultimate compressive capacity of full-scale specimens which represent an actual part of large bilge strake panel in an existing pilot boat. A universal test machine with computerized system and capacity of 2000 kN is used for conducting the compressive test as shown in [Figure 2](#). An arrangement similar to that adopted by Saad eldeen et al. [3] has been applied, where the panel specimen is located at the centre of the test machine between two heavy supporting clamps with a thickness and depth of 20mm and 50mm, respectively, designed with two gaps for the attached stiffeners to facilitate the replacement of the panels as may be seen in [Figure 2](#). The short edges of the panels are restrained within the depth of the supporting clamps using bolt connections. The supporting clamps are assumed to constrain rotation and lateral displacement throughout their depth. The test has been conducted with displacement rate of 0.016mm/s and both vertical displacement as well as the acting load is recorded by the testing machine. The applied load is transmitted to the tested panel a thick plate in order to insure the uniform distribution of the acting load. An additional mechanical displacement gauge is fitted on the centre of the specimen for measuring the lateral displacement as presented in [Figure 2](#).

### 2.1.1. Panel Geometrical Configurations

The basic geometrical configurations of the tested panels shown in [Figure 3](#) are part of real pilot structure, where the plate thickness is 6 mm with two flat bar attached stiffener 60×6 mm by means of fillet staggered welding. Both plates and stiffeners are fabricated from wrought aluminium alloy 5083-H116 and GMAW technique is used for the welding process with 1.2mm diameter electrode wire fabricated from aluminium alloy 5653. According to the geometrical configurations as well as the real mechanical properties, the plate and column slenderness of the panel are 2.74 and 0.526 respectively,

according to the expression given by Eq.3 and Eq.4. [4]

$$\beta = b/t \sqrt{\frac{\sigma_y}{E}} \quad (3)$$

$$\lambda = L/r \sqrt{\frac{\sigma_y}{E}} \quad (4)$$

$\beta$  is the plate slenderness,  $b$  is the plate breadth,  $t$  is the plate thickness,  $\sigma_y$ ,  $E$  are the material yield strength, and Young modulus,  $\lambda$  is the column slenderness,  $L$  is panel length,  $r$  is the radius of gyration,  $r = \sqrt{I/A}$ ,  $I$  and  $A$  are the moment of inertia and the area of the stiffener cross-section. To study the effect of through thickness crack; several locked crack locations and orientations are produced with crack length of 80 mm, between the two stiffeners as presented in [Table 2](#) and [Figure 4](#). A laser cutting machine with a cutter diameter 2mm is used to produce the cracks, to minimize deformation and residual stresses.

As given in [Table 2](#) and [Figure 4](#), the panel specimens are denoted as SP-intact for intact panel (no cracks), SP-LC panel with longitudinal/central crack, SP-LU panel with longitudinal/upper quarter crack, SP-AC panel with angular /central crack and SP-AU panel with angular/upper quarter crack. Before conducting the collapse tested of the welded aluminium panels, a survey of initial imperfection measurements has been performed.

**Table 1: Tensile tests results of aluminum alloy AA5083-H116**

Item	Youngs Modulus E (GPa)	Elastic Limit (MPa)	Ultimate tensile strength (MPa)
Engineering	63	150	320
True	63	150.372	360

The observed shapes and amplitudes of the initial imperfections of the analysed panels are summarized and illustrated in [Table 3](#) and [Figure 5](#). It was observed that all panels follow one initial shape as presented in [Figure 5](#), but with different imperfection amplitudes  $w_1$  and  $w_2$ . For instance, the intact panel SP-intact has a symmetric imperfection amplitude  $w_1 = w_2 =$

10 mm, while the panel with angular/central crack SP-AC is of asymmetric imperfection amplitude of  $w_1=4$  mm and  $w_2=7$  mm.

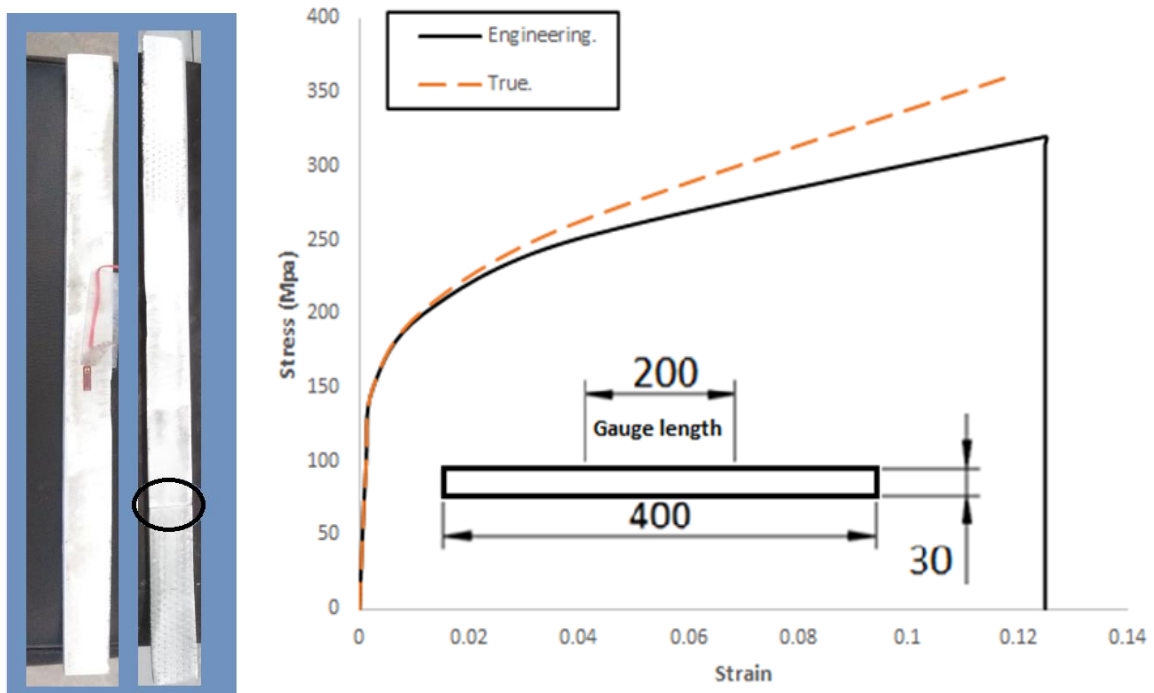


Figure 1: A rectangular tested coupon (left) and engineering and true stress-strain relationship (right)

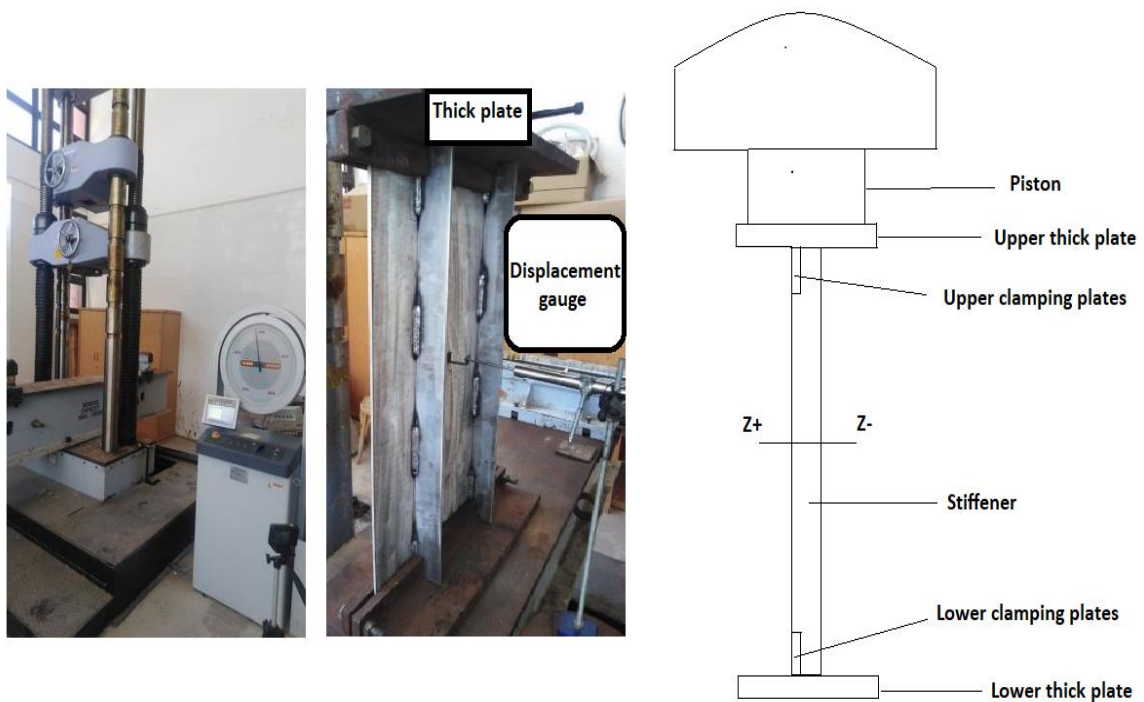
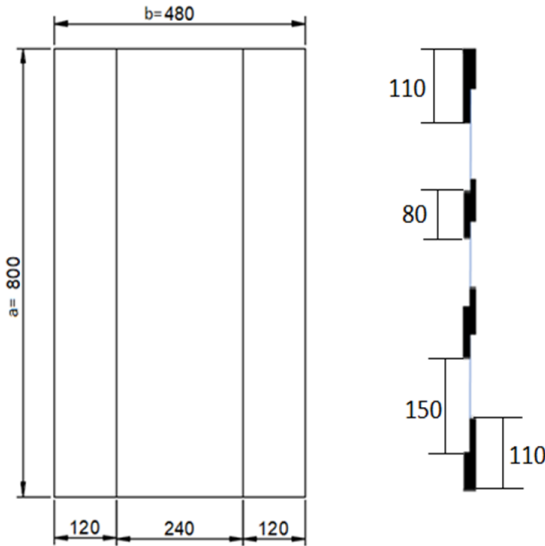


Figure 2: Experimental test setup, Structure and Concrete Research Laboratory, Faculty of Engineering, Port Said University

**Table 2: Geometrical configurations of the tested panel**

Item	Crack length (mm)	Crack position X, Y (mm)	Crack orientation
SP-intact	----	----	----
SP-LC	80	X=400; Y=240	90°
SP-LU	80	X=640; Y=240	90°
SP-AC	80	X=400; Y=240	70°
SP-AU	80	X=640; Y=240	70°



**Figure 3: Basic geometry of the tested panel.**

### 3. EXPERIMENTAL RESULTS

The compressive test has been conducted in one loading cycle to find out the ultimate capacity of intact and cracked stiffened panels and to analyse the behaviour of each panel with respect to the applied compressive load.

**Table 3: Amplitudes of the specimens imperfections**

Specimen	w1 (mm)	w2 (mm)
SP-intact	10	10
SP-LC	14	14
SP-LU	8	10
SP-AC	4	7
SP-AU	8	8

#### 3.1. Intact Panel, SP-intact

Before conducting the collapse test, the observed initial imperfection of the SP-intact panel is symmetric with upward amplitude 10 mm of the frontier plate, as described in Figure

5 and Table 2, where the plate between the attached stiffeners is almost flat. The collapse mode for the intact panel is shown in F. The collapse is reached at an ultimate load of 430.4 kN as shown in load-shortening curve Figure (left). It may be noticed from F that both stiffeners registered out of plane deformation (outward). The reason for such deformation is the failure of the plate at such specific location represented by downward deformation that forces the stiffener to buckle outward. This results in welding damage and plate separation as may be seen from the specimen details at point (1,2) for the first stiffener S1 and points (3,4) for the second stiffener S2, see Figure 6. This failure mode results in a gap between the plate and the attached stiffeners. It may be noticed that the final deformed shape of the plating is complex and asymmetric. The registered axial displacement by the testing machine as well as the applied load is presented in Figure 7 (left), in which the pre-buckling regime ends at 166 kN with shortening displacement 0.69 mm. The intact panel, SP-intact registered ultimate compressive capacity of 430.4 kN with corresponding axial shortening displacement 3.48mm. Based on the recorded lateral displacement during the experiment using a mechanical displacement gauge mounted at the mid-length-breadth of the specimen, the relationship between the axial load and the lateral displacement is presented in Figure 7 (right). It may be noticed that from the beginning of loading the middle portion of the panel buckled in the upward direction with a lateral displacement of 4.7 mm with respect to the ultimate load carrying capacity.

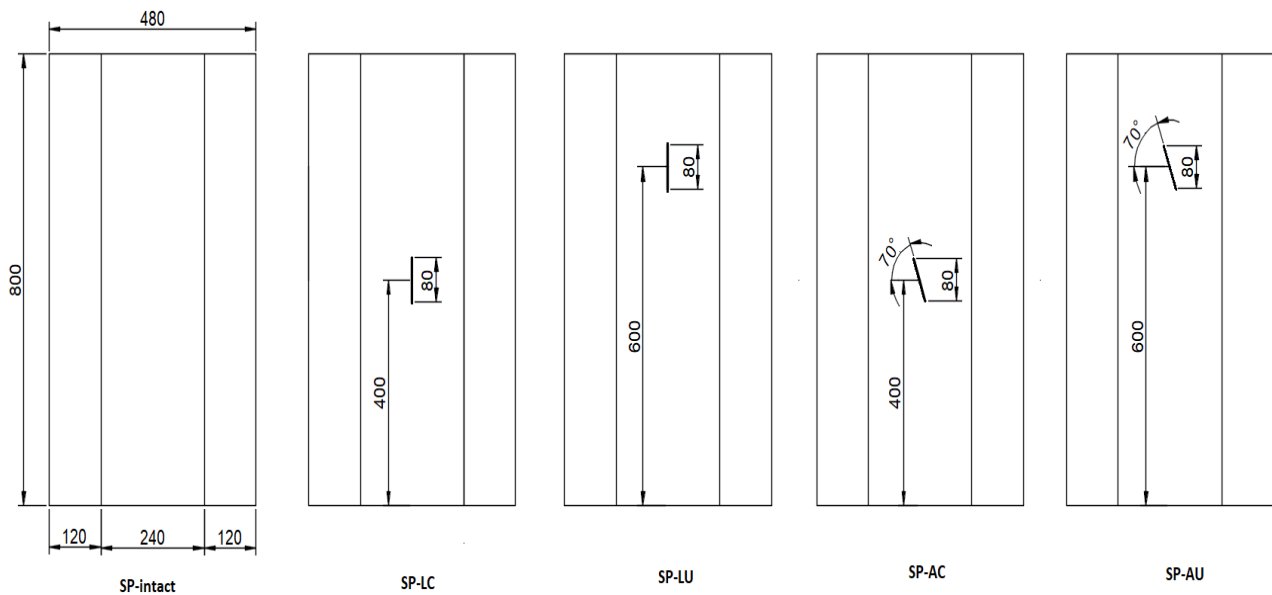


**Figure 4: Geometrical configuration of the tested aluminum stiffened panels**

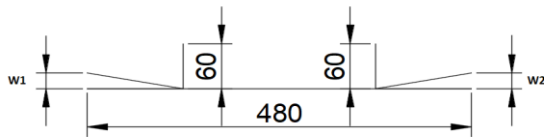


**Figure 5: Description of the observed initial imperfections of the analyzed panels**

### 3.2. Stiffened panel with longitudinal center crack, SP-LC

The panel specimen SP-LC has a longitudinal central crack in the direction of loading with length of 80 mm. The initial imperfection shape is symmetric with imperfection amplitude of 14 mm as given in Table 3. The final collapse mode after removing the applied load is shown in Figure 8. It may be noticed that the deformed shape of the stiffeners is symmetric with inward tripping, which results from the downward buckling of the plate between the attached stiffeners. This is followed by welding damage of stiffener S2 at the location shown in Figure 8 and on contrary, no welding damage occurs for the first stiffener S1. It may be noticed that the developed deformation for both plating and stiffeners occurred far from the existing crack and close to the upper clamp, which may result in lower axial compressive capacity of 379.72 kN, in addition to the higher symmetric initial imperfection of 14 mm, which may facilitate the

occurrence of earlier buckling. The developed vertical displacement; shortening with respect to the applied load is shown in Figure 9 (left), where the panel SP-LC recorded ultimate compressive capacity of 379.72 kN, with shortening displacement of 2.04 mm. It may be noticed that the elastic response of the panel ends at 199.07 kN with corresponding displacement of 0.79 mm. As may be seen in Figure 9 (left) a sudden decrease in the load carrying capacity occurred simultaneously with the failure of the plate to withstand the applied load, followed by welding damage and then stiffeners tripping.

Figure 9 (right) represents the relationship between the measured lateral displacement using the displacement gauge and the acting load, it is evident that the middle portion of the panel SP-LC at which the measurements are recorded buckled downwards from the beginning of loading, recording lateral displacement at the ultimate loading capacity of -1.76mm.



Figure 6: Collapse shape of the intact panel

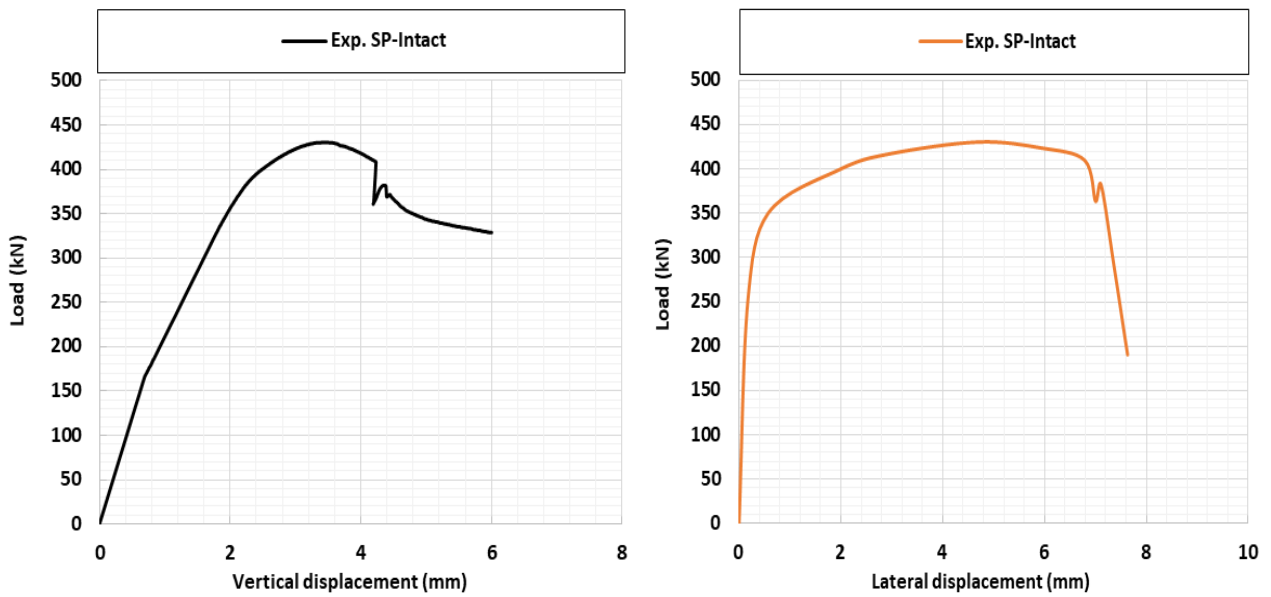


Figure 7: Load shortening (left) and load-lateral displacement (right), SP-intact



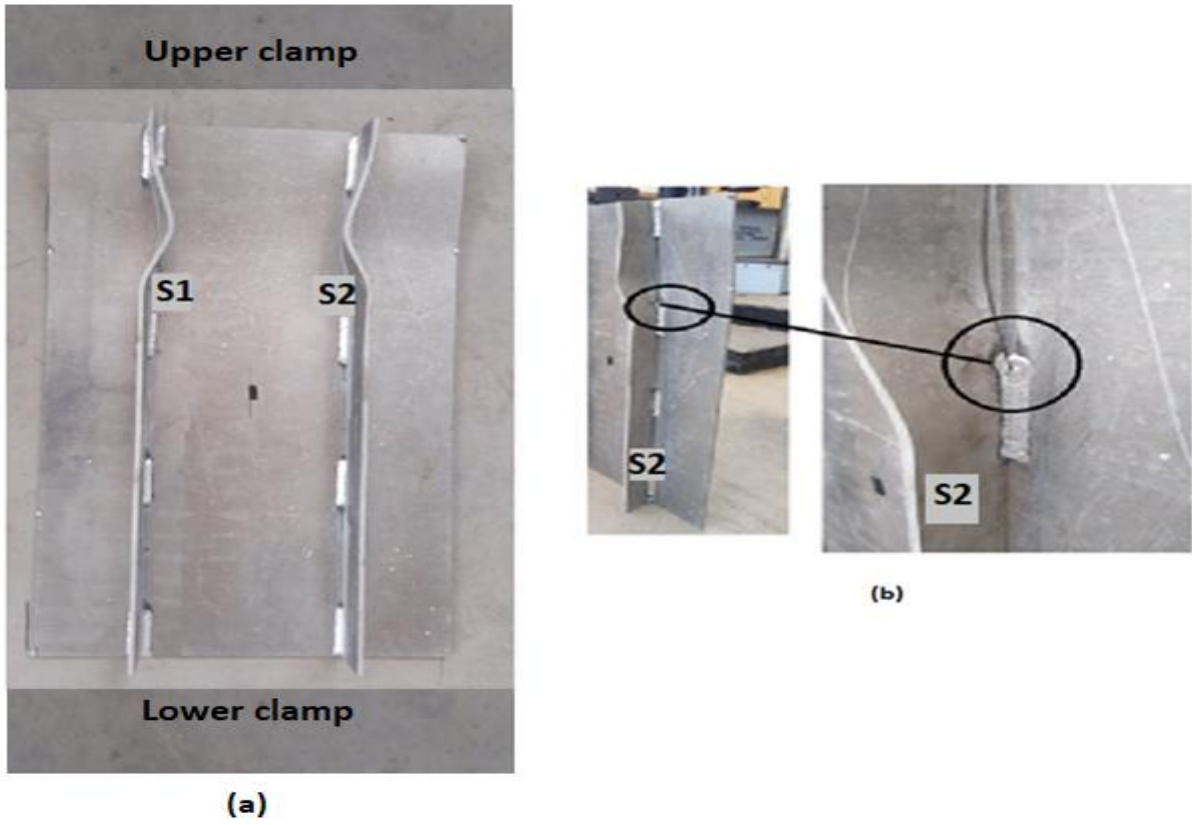


Figure 8: Collapse shape of SP-LC

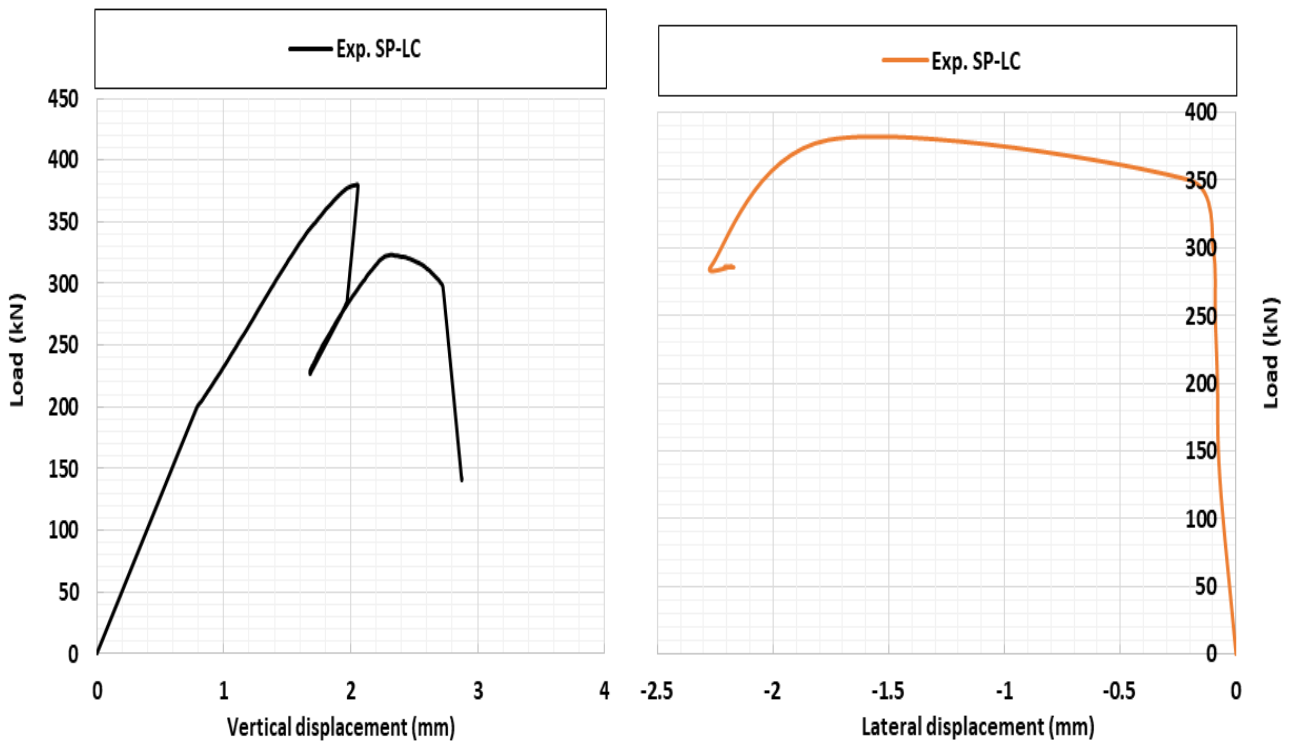


Figure 9: Load shortening (left) and load-lateral displacement (right), SP-LC

### 3.3. Stiffened Panel with Longitudinal Upper Quarter Crack, SP-LU

The crack for the present panel is a longitudinal crack of length 80 mm and located at the upper quarter of the panel SP-LU, as described in Figure 4 and Figure 10. Before the compressive test, the measured initial imperfection indicates that it is of symmetric shape with different amplitudes of 8 and 10 mm for  $w_1$  and  $w_2$ , respectively, as given in Table 3 and shown in Figure 5. As may be seen from Figure 10, the panel failed with inward deformation of both stiffeners near the lower clamp and far from the location of the crack without triggers of welding damage. Also, it may be noticed that the first stiffener S1 tripped inward with higher amplitude than the second stiffener S2. Therefore, it is evident that the final collapse mode of such panel is asymmetric. This deformed shape in addition to the undamaged welding affect directly the total capacity of the panel, where a high load carrying capacity of 504.8 kN is registered, with relevant shortening displacement of 3.32 mm, as presented in Figure 11 (left). After reaching the ultimate load, a sharp discharge of the capacity occurs without any recovery. Figure 11 (right) represents the relationship between the applied load and the developed lateral displacement at the center of the panel, it is clear that from the beginning of loading the central part between the two stiffeners deformed upward with lateral displacement related to the ultimate capacity of 0.1mm.

### 3.4. Stiffened Panel with Angular Central Crack, SP-AC

For this panel, the central crack is oriented with  $\theta=70^\circ$  as shown in Figure 4, and before loading the geometrical imperfection of the plating is of symmetric shape, but the amplitude is different;  $w_1=4$  mm and  $w_2=7$  mm, see Table 3. As may be seen from Figure 12, the panel collapsed asymmetrically in both plating and stiffeners, resulting in higher ultimate compressive capacity of 508 kN. During the test, cracking weld damage was noticed for

stiffener S1 as presented in F, due to the failure of the plate to withstand the applied load near the upper clamp, which forces S1 to deform. After that the second stiffener S2 failed to carry the acting load, and responded with outward tripping at the mid-span of the panel aligned with the crack. The load-shortening relationship is presented in Figure 13 (left), where the global elastic behavior of SP-AC panel ends at acting compressive load of 240.4 kN, with elastic shortening of 1.08 mm. After that the permanent deformation of the plate beneath the S1 at the location of damage presented in F occurs, which forces the panel to a partial loss of capacity after reaching the ultimate load at 508 kN, followed by plate resistance to the applied load, until the second stiffener tripped outward at a lower load of 499.2 kN with maximum amplitude aligned transversely with the crack location, as may be seen in Figure 13 (left). The lateral response of the plate between the attached stiffeners is presented in F (right) by the lateral displacement versus the acting load.



Figure 10: Collapse shape of specimen SP-LU

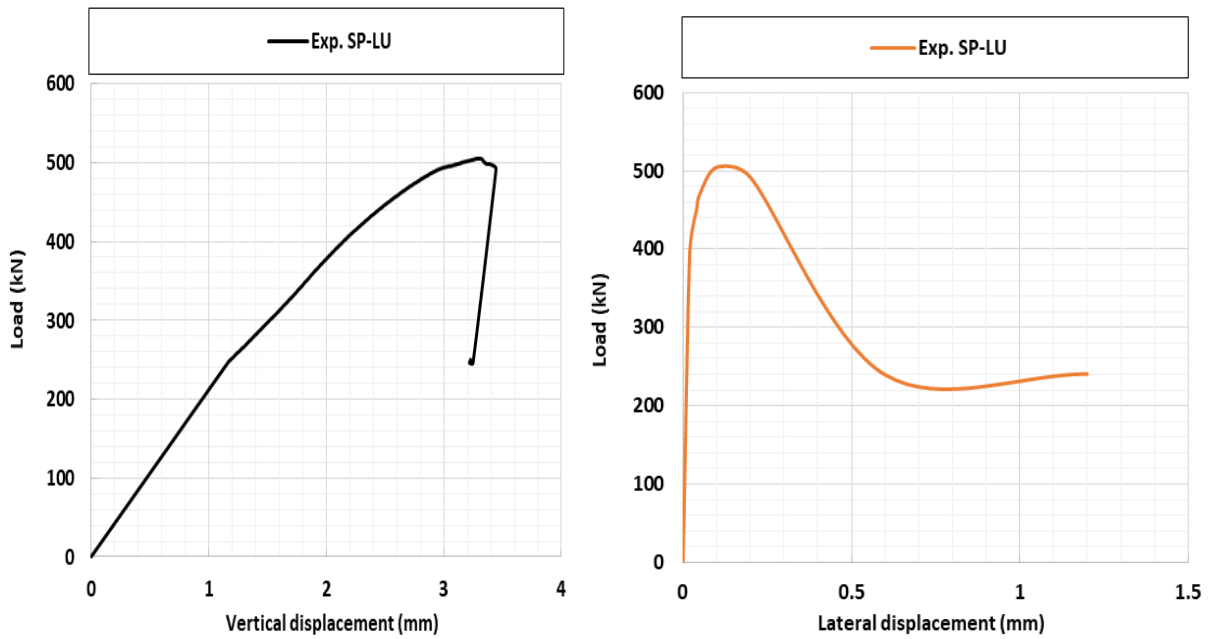


**Figure 11: Load shortening (left) and load-lateral displacement (right), SP-LU**

It is evident that till 400 kN, no change with respect to the original initial imperfection of the middle portion is registered. At the ultimate load, the panel registered a slight upper deflection of amplitude 0.01 mm and increases with increasing the capacity discharge. This may be explained by the contribution of the angular central crack to the stability of the middle portion until the second stiffener S2 and the corresponding plate failed to withstand the applied load, see Figure 12.

### 3.5. Stiffened Panel with Angular Upper Quarter Crack, SP-AU

For the current panel SP-AU, the crack is located at the center of the upper quarter of the panel with  $\theta=70^\circ$  of orientation as described in Figure 4. The developed collapse mode of the panel is asymmetric including plate and stiffeners see F, regardless of the symmetric initial imperfection shape and amplitude of 8 mm as reported before the compressive test, see Table. As may be seen form F, (left), the deformation occurs at the frontier plate near the center of the panel and beneath the first stiffener S1, which forces S1 to trip outward and reach the ultimate capacity of 446 kN as presented in F (left). After that the capacity discharged with capacity reserve at 320.4 kN

until the progressive collapse of the second stiffener S2 in line with the angular crack location and near the upper clamp occurred, followed by plate buckling, see Figure 14, (right) and failure of the panel. It has to be stated that despite the absence of welding damage, SP-AU panel registered lower load carrying capacity compared to the panel with angular central (SP-AC) which reported welding damage as shown in Figure 12. The reason may be related to the difference in the initial imperfection shape of both panels, noting that SP-AU has a symmetric imperfection shape which is considered to be the weakest shape of the initial imperfection to resist the compressive load as concluded by [16]. Also, the occurrence of damage near the upper clamp and close to the crack location may decrease the structural capacity of the panel as noted in SP-AU. The relationship between the lateral displacement and the acting vertical load is presented in Figure 15 (right), in which the location of the mechanical displacement gauge shows upward lateral displacement with some disturbance between 132 kN and 246 kN, which is the end of the elastic regime. After that the lateral displacement increases as the acting load increases, registering lateral displacement with respect to the ultimate capacity on 1.48 mm.

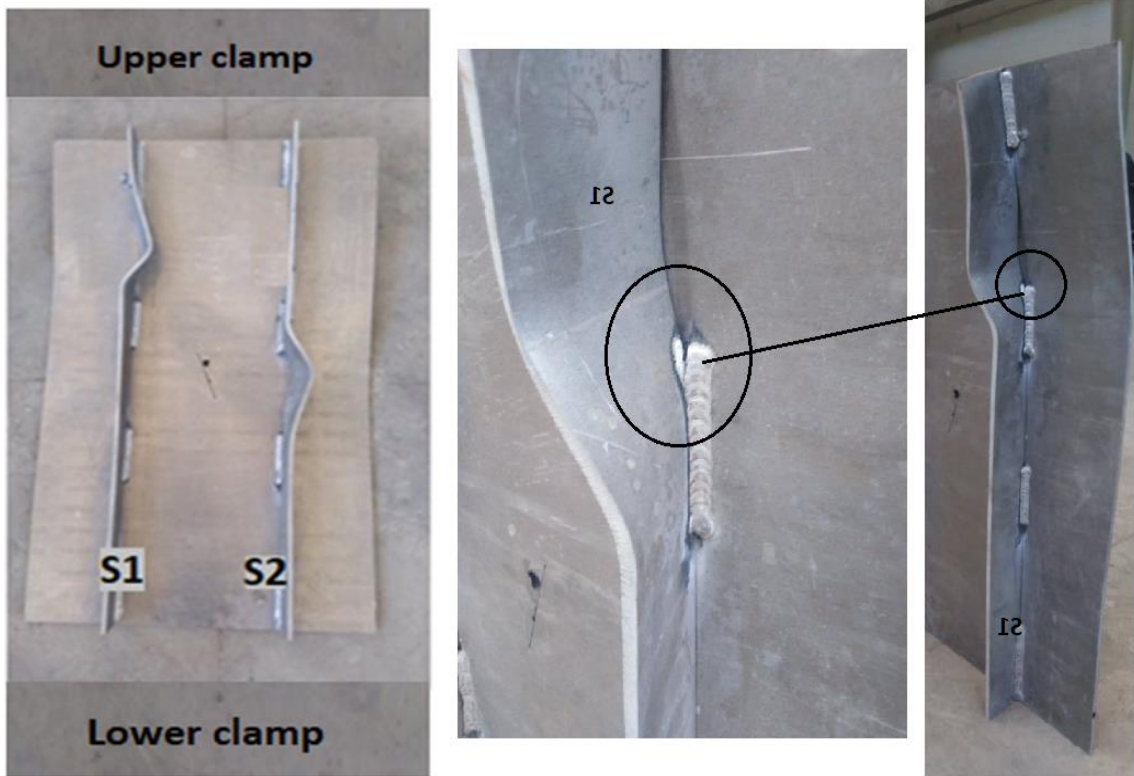


Figure 12: Collapse shape of specimen SP-AC

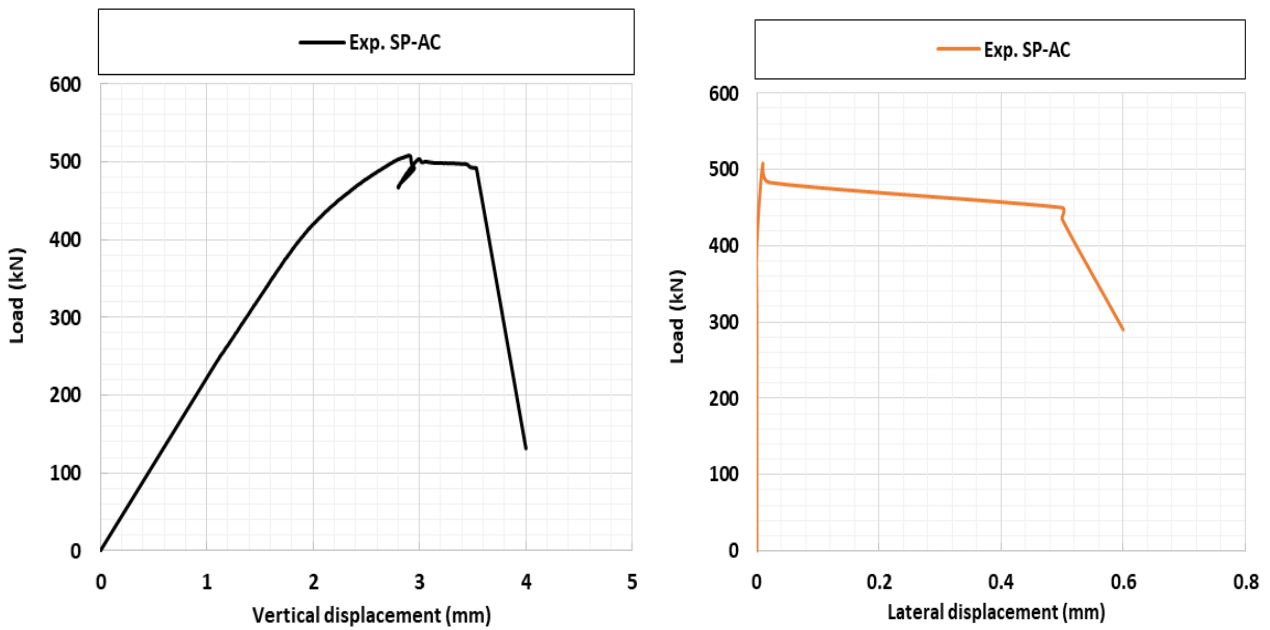


Figure 13: Load shortening (left) and load-lateral displacement (right), SP-AC



Figure 14: Collapse shape of specimen SP-AU during the test (left) and after (right).

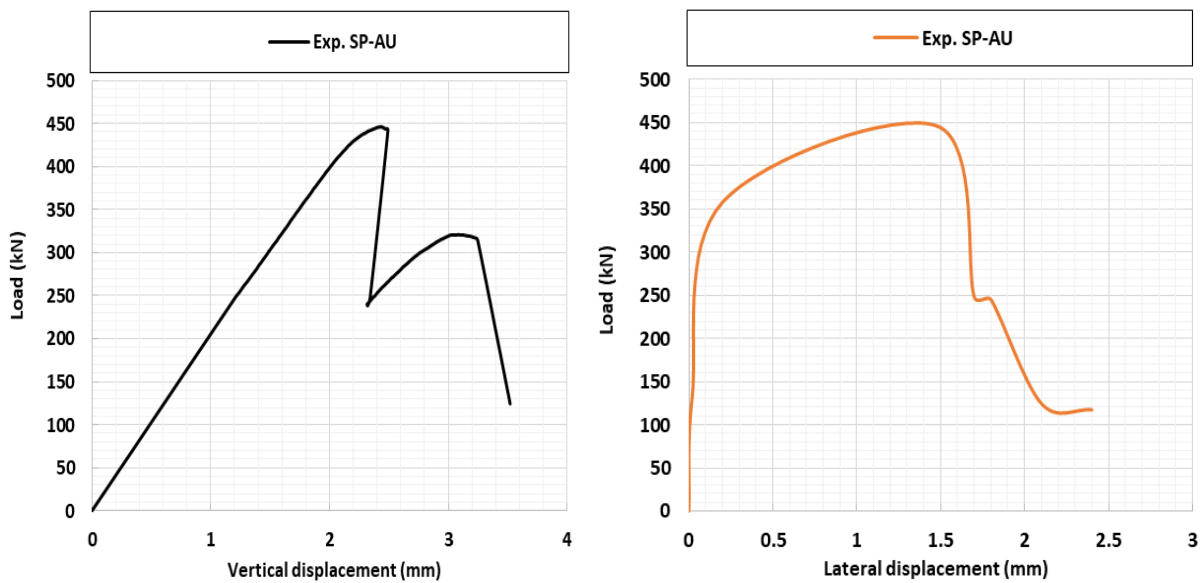


Figure 15: Load shortening (left) and load-lateral displacement (right), SP-AU

## 4. DISCUSSION OF RESULTS

The results obtained for the tested specimens are compared to each other to find out the effect of crack location and orientation with respect to the intact panel, taking into consideration the effect of initial imperfections.

### 4.1. Structural Response of Panels with Different Crack Locations

In this subset of the analysis, the effect of the crack location on the ultimate compressive capacity as well as on the collapse mode will be discussed for SP-Intact, SP-LC and SP-LU. The load-shortening curve for the three panels is presented in Figure 16 (left), with the corresponding ultimate values in Table 4.

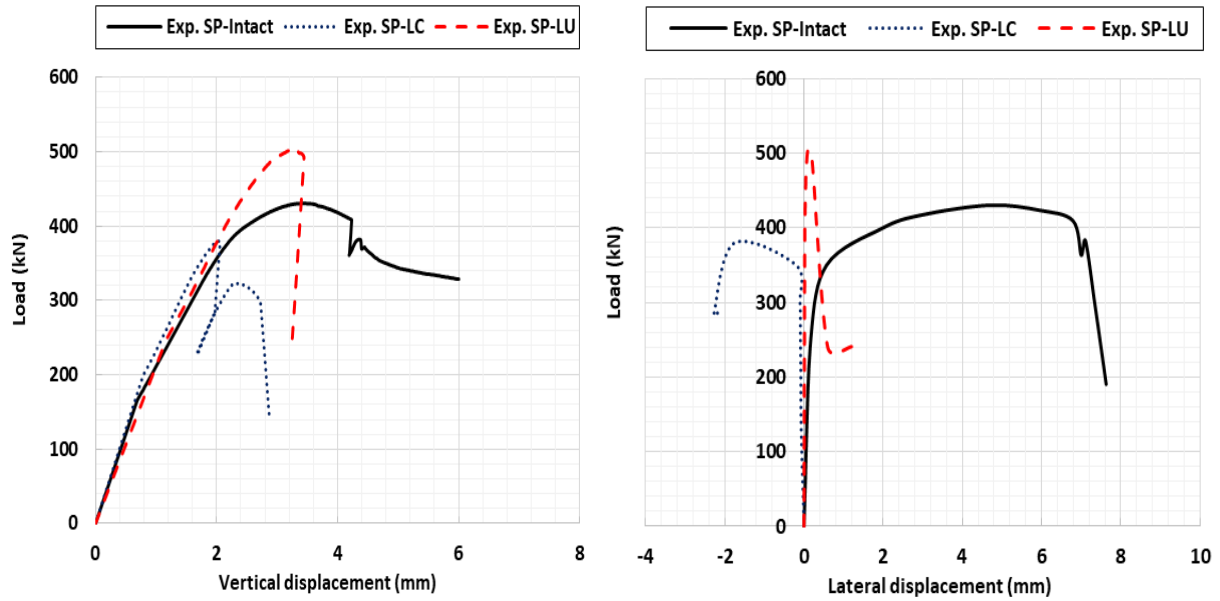


Figure 16: Load-shortening (left) and load-lateral displacement (right), considering different crack locations

Table 4: Ultimate compressive capacity, shortening and lateral displacement; different crack locations.

Specimen	Ultimate capacity (kN)	Shortening displacement (mm)	Lateral displacement (mm)
SP-intact	430.4	3.48	+4.7
SP-LC	379.72	2.04	-1.76
SP-LU	504.8	3.32	+0.1

From ultimate capacity point view, it appears that both panels SP-LC and SP-LU registered different responses with respect to SP-Intact, where SP-LC collapsed with lower capacity than the intact one by 11.78%, on contrary to SP-LU, where higher capacity than the intact one was registered by 17.29%, see Figure 16 (left) and Table 4. The primary reason for such difference responses may be due to the initial imperfection, where the panel SP-LC had a high plating symmetric amplitude 14 mm; this panel developed a final downward lateral central displacement of -1.76 mm, that facilitates the earlier capacity discharge, in

addition to the occurrence of stiffeners tripping near the upper clamp, with a shortening displacement of 2.04 mm which is less than the intact one. On contrary, the capacity of the panel SP-LU seems to be enhanced by the asymmetric initial imperfection of amplitudes 8 mm and 10 mm; this remark is supported by the final upward lateral displacement of 0.1 mm, see Figure 16 (right), which is in agreement with the work done by Saad Eldeen et al. [3] who concluded that the sign of the imperfection amplitude as well cracks governs final the collapse shape and mode and provides more carrying capacity.

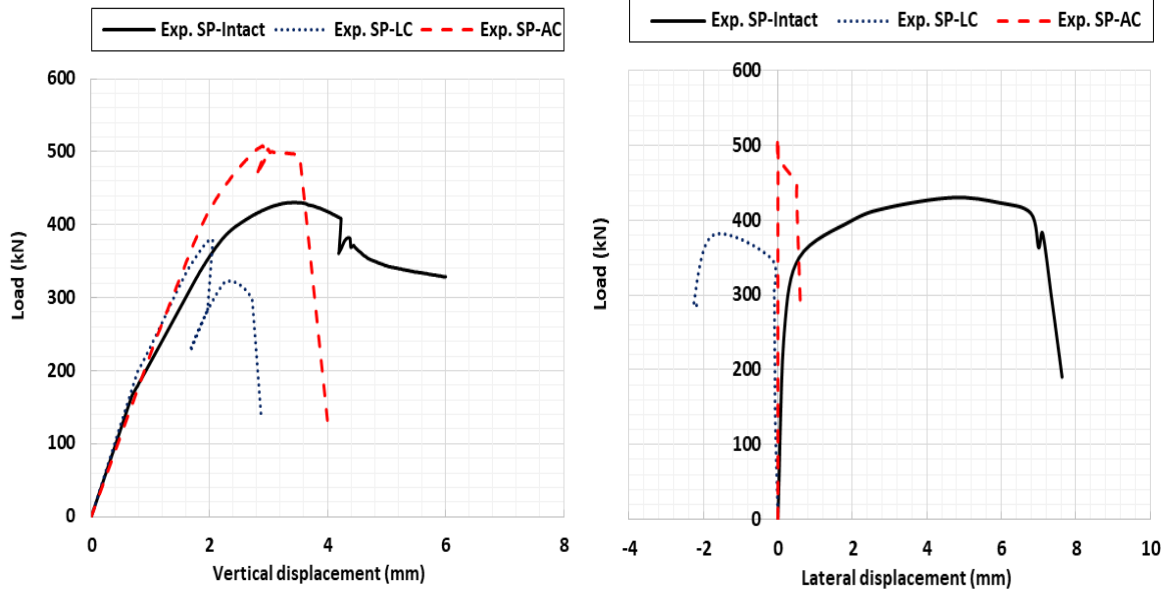


Figure 17: Load-shortening (left) and load-lateral displacement (right), considering central crack orientation

Table 5: Ultimate compressive capacity, shortening and lateral displacement; central crack orientation

Specimen	Ultimate capacity (kN)	Shortening displacement (mm)	Lateral displacement (mm)
SP-intact	430.4	3.48	+4.7
SP-LC	379.72	2.04	-1.76
SP-AC	508	2.90	+0.01

Stiffeners' tripping occurred far from the acting point (near the lower clamp), and the resulting shortening displacement is 3.32 mm. It has to be stated that for both locked cracked panels SP-LC and SP-LU, the failure of plating and stiffeners occurs away from the crack location, which in turn reduces the possibility that locked crack location could have affected the global capacity.

#### 4.2. Structural Response in Case of Central Crack Orientation

The response of the panels SP-LC and SP-AC for different central crack orientation with respect to the intact panel SP-Intact will be investigated. As may be seen from Figure 17 (left), both panels behave in different manner with respect to the intact panel as previously stated for different crack location. For SP-AC panel with crack orientation  $\theta=70^\circ$ , the ultimate capacity is higher than the intact one

by 18.03%, see Table 5, which may result from the asymmetric initial imperfection amplitudes of 4 mm and 7 mm, which are less than both intact and SP-LC panels, followed by almost flat final lateral displacement 0.01 mm, see Figure 17 (right). It was noticed that, for SP-AC panel, the tripping of the second stiffener S2 is aligned with the angular crack creating an asymmetrical deformation of the two stiffeners.

#### 4.3. Structural Response in Case of Upper Quarter Crack Orientation

For this subset of the analysis, the response of the panel with locked cracks located at the upper quarter with different orientation SP-LU and SP-AU will be analyzed. It may be noticed that, both panels SP-LU and SP-AU withstand ultimate capacity higher than the intact one by 17.29% and 3.62%, respectively, see Figure 18 (left) and

Table 6, which is on contrary to the panels with central crack. For SP-AU panel, there are several remarks which result in higher capacity than the intact one as the less symmetrical imperfection amplitude of 8mm, compared to the intact panel of 10 mm. Also, the less developed final lateral displacement of 1.48 mm, where the intact one is 4.47 mm as presented in Figure 18 (right). Furthermore, no welding damage occurs for SP-AU, but for the intact panel, four locations of welding damage were reported as may be seen from the collapse shape in Figure 6, which directly affects the capacity of the intact panel. From stiffeners

tripping point of view, it may be noticed that the deformation mode is almost the same with outward tripping of the two stiffeners, with central tripping of S1 and near the upper clamp for S2 as described in Figure 6 and Figure 14. The observation regarding the alignment of the tripping of the second stiffeners to the angular crack is noticed in for SP-AU, in the same way of SP-AC panel. Therefore, it may be stated that the orientation of the crack may affect the final deformation mode of any of the nearest stiffeners, which is on contrary to the longitudinal crack in spite of the crack location.

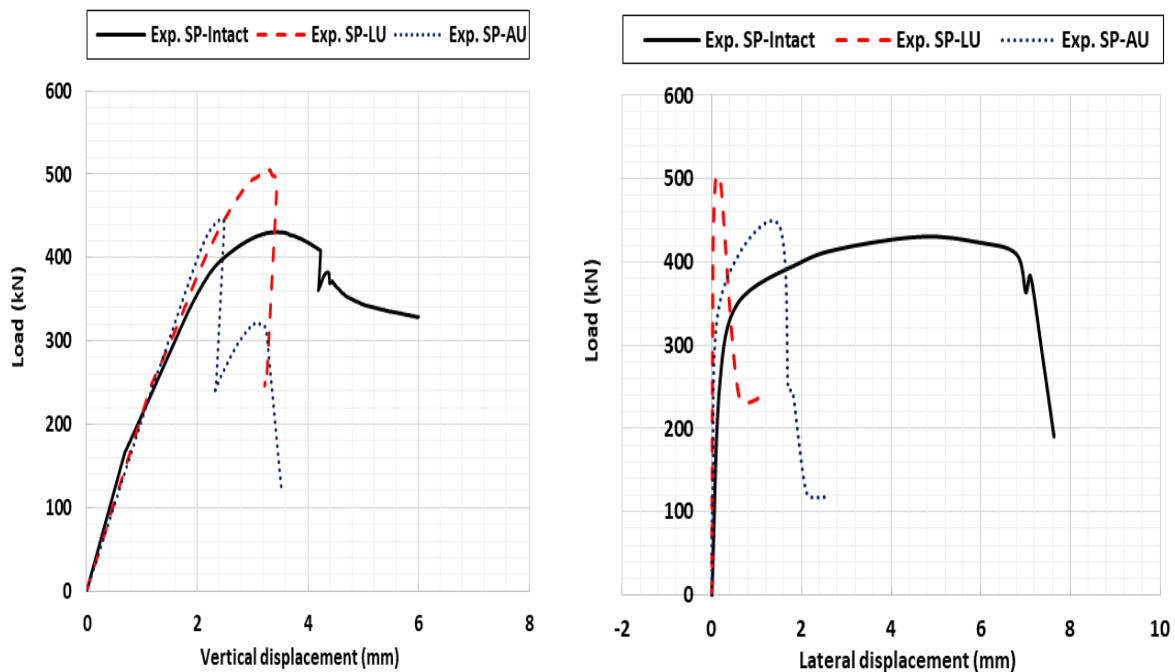


Figure 18: Load-shortening (left) and load-lateral displacement (right), considering upper quarter crack orientation

Table 6: Ultimate compressive capacity, shortening and lateral displacement; upper quarter crack orientation

Specimen	Ultimate capacity (kN)	Shortening displacement (mm)	Lateral displacement (mm)
SP-intact	430.4	3.48	+4.7
SP-LU	504.8	3.32	+0.1
SP-AU	446	2.43	+1.48



The increase in their load-carrying capacity may be related to the state of initial imperfections which is known to be of predominant effect [16]. The comparison of all values and curves does not indicate clear relationships regarding the location and orientation of the cracks produced.

## 5. CONCLUSIONS

A series of experimental tests of full scale welded stiffened aluminum panels in alloy 5083-H116 with and without locked cracks is conducted under uniaxial compressive loading. The locked cracks are located in either in the center or the upper quarter with different orientation. Based on the performed analysis, the following remarks may be stated; for the applied weld type, the occurrence of initial failure of the plating in opposite direction to the stiffeners forces the weld to be damaged and facilitates the occurrence of earlier tripping of the stiffeners, resulting in quick loss of the global capacity.

The asymmetric initial imperfection amplitude accompanied by final upward lateral displacement may enhance the structural capacity, in addition to the occurrence of stiffeners tripping far from the acting point. For panels with longitudinal crack, the failure of plating and stiffeners occurs away from the crack location, which in turn reduces the possibility that locked crack location could have affected the global capacity. The occurrence of damage near the upper clamp and close to the crack location may decrease the structural capacity of the panel conditionally that the final collapse mode is of symmetric shape. It may be stated that the orientation of the crack may affect the final deformation mode of any of the nearest stiffeners, which is on contrary to the longitudinal crack is not affected by the crack location. The present experimental work may effectively contribute in the development and validation of a numerical model in order to study the effect of all crack characteristics on the ultimate strength of aluminum panels used in marine industry. Further experimental tests

taking into consideration different crack lengths, locations, and orientations, in addition to different welding types would give a better insight of the effect of cracks on the ultimate strength of stiffened aluminum panels.

## Declaration of Competing Interest

The authors declare that they have no known competing financial interests or personal relationships that could have appeared to influence the work reported in this paper.

## ACKNOWLEDGMENT

The authors would like to express their gratitude to the Commander of the Egyptian Navy for his support to provide the full-scale specimens fabricated in The Navy Shipyard in Alexandria, and to Dr. Ezzaat A. Sallam for his technical support to perform the tests in the Structure and Concrete Research Laboratory, Faculty of Engineering, Port Said University.

## ABBREVIATIONS

FSW: Friction stir welding.

GMAW: Gas metal arc welding.

MIG: Metal inert gas.

## CREDIT AUTHORSHIP CONTRIBUTION STATEMENT:

Ashraf Attia: Experiments, Analysis and Editing, S. Saad-Eldeen: Concept, Methodology and Reviewing, Mostafa M. EL-Afandy: Concept, Methodology and Reviewing, H.S. El-Kilani: Concept, Methodology and Reviewing.

## REFERENCES

- [1] Paik, J.K., C. Andrieu, and H.P. Cojeen, Mechanical collapse testing on aluminum stiffened plate structures for marine applications. *Marine Technology and SNAME News*, 2008. **45**(04): p. 228-240.
- [2] Saad-Eldeen, S., Y. Garbatov, and C.G. Soares, Experimental investigation on the residual strength of thin steel plates with a central elliptic opening and

- locked cracks. *Ocean Engineering*, 2016. **115**: p. 19-29.
- [3] Saad-Eldeen, S., Y. Garbatov, and C.G. Soares, Experimental strength analysis of steel plates with a large circular opening accounting for corrosion degradation and cracks subjected to compressive load along the short edges. *Marine Structures*, 2016. **48**: p. 52-67.
- [4] Shi, X.H., J. Zhang, and C.G. Soares, Experimental study on collapse of cracked stiffened plate with initial imperfections under compression. *Thin-Walled Structures*, 2017. **114**: p. 39-51.
- [5] Zhang, J., et al., Ultimate strength of stiffened panels with a crack and pits under uni-axial longitudinal compression. *Ships and Offshore Structures*, 2020: p. 1-20.
- [6] Yu, C.L., et al., Ultimate strength characteristic and assessment of cracked stiffened panel under uniaxial compression. *Ocean Engineering*, 2018. **152**: p. 6-16.
- [7] Xu, M.C., Y. Garbatov, and C.G. Soares, Residual ultimate strength assessment of stiffened panels with locked cracks. *Thin-Walled Structures*, 2014. **85**: p. 398-410.
- [8] Rahbar-Ranji, A. and A. Zarookian, Ultimate strength of stiffened plates with a transverse crack under uniaxial compression. *Ships and Offshore Structures*, 2014. **10**(4): p. 416-425.
- [9] Aalberg, A., M. Langseth, and P. Larsen, Stiffened aluminium panels subjected to axial compression. *Thin-walled structures*, 2001. **39**(10): p. 861-885.
- [10] Farajkhah, V. and Y. Liu, Effect of fabrication methods on the ultimate strength of aluminum hull girders. *Ocean Engineering*, 2016. **114**: p. 269–279.
- [11] Hosseinabadi, O.F. and M.R. Khedmati, A review on ultimate strength of aluminium structural elements and systems for marine applications. *Ocean Engineering*, 2021. **232**: p. 109153.
- [12] Liu, B., et al., Strength assessment of aluminium and steel stiffened panels with openings on longitudinal girders. *Ocean Engineering*, 2020. **200**: p. 107047.
- [13] Duan, F., et al., Dynamic behaviour of aluminium alloy plates with surface cracks subjected to repeated impacts. *Ships and Offshore Structures*, 2019. **14**(5): p. 478-491.
- [14] Attia, A., H.S. El-Kilani, and S. Saad-Eldeen. Ultimate Strength Behavior of Cracked Ship Panels: a Review. in *International Conference on Offshore Mechanics and Arctic Engineering*. 2021. American Society of Mechanical Engineers.
- [15] Dieter, G.E. and D.J. Bacon, *Mechanical metallurgy*. Vol. 3. 1976: McGraw-hill New York.
- [16] Guedes Soares, C. and T. Søreide, Behaviour and design of stiffened plates under predominantly compressive loads. *International Shipbuilding Progress*, 1983. **30**(341): p. 13-27.